AD-A049 085 CAMBRIDGE ACOUSTICAL ASSOCIATES INC MASS F/G 20/1
RADIATION IMPEDANCE FOR THE ELEMENTS OF A CYLINDRICAL TRANSDUCE--ETC(U)
APR 60 R V WATERHOUSE NONR-2739(00)

UNCLASSIFIED NL

1 OF 1
ADA049 085

END
DATE FILMED
3-78
DDC

(1)

CODE 411

FILE COPY

CAMBRIDGE ACOUSTICAL ASSOCIATES, INC.

CONSULTANTS IN ACOUSTICS AND DYNAMICS

1278 MASSACHUSETTS AVENUE, CAMBRIDGE 38, MASSACHUSETTS





# RADIATION IMPEDANCE FOR THE ELEMENTS OF A CYLINDRICAL TRANSDUCER IDEALIZED AS AN OBLATE SPHEROID

A Technical Report

Prepared for

The Department of the Navy
Office of Naval Research
Under Contract Nonr-2739(00)

by

Richard V. Waterhouse



8 April 1960

31 August 1960

TO: Office of Naval Research (Code 411)
Department of the Navy
Washington 25, D. C.

FROM: CAMBRIDGE ACOUSTICAL ASSOCIATES, INC.

RE: Erratum for "Radiation Impedance for the Elements of a Cylindrical Transducer Idealized as an Oblate Spheroid," by R. V. Waterhouse, A Technical Report Prepared for Office of Naval Research, Contract Nonr-2739(00), 8 April 1960.

On page 14, the integrand of the integral $\int_{\eta_{j1}}^{\eta_{j2}}$ should be multiplied by the product of the scale factors $h_\eta(\xi_o,\eta)$ and $h_\varphi(\xi_o,\eta)$. Equation 8.1 now reads:

$$Z_{ij} = \frac{1}{u} \sum_{m,n} \int_{\eta_{j1}}^{\eta_{j2}} \int_{\varphi_{j1}}^{\varphi_{j2}} P_{mni}(\xi_o,\eta,\varphi) h_\eta(\xi_o,\eta) h_\varphi(\xi_o,\eta) d\varphi d\eta$$

The integral $\int_{\eta_{j1}}^{\eta_{j2}} S_{mn}(\eta)d\eta$ in Eqs. 8.2 and 8.3 is now replaced by the integral:

$$\left(\frac{d}{2}\right)^2 \left(\xi_o^2+1\right)^{\frac{1}{2}} \int_{\eta_{j1}}^{\eta_{j2}} \left(\xi_o^2+\eta^2\right)^{\frac{1}{2}} S_{mn}(\eta)d\eta$$

It is seen that the product of the two integrals $\int_{\eta_{i1}}^{\eta_{i2}}$ and $\int_{\eta_{j1}}^{\eta_{j2}}$ can now be written explicitly as follows, after substitution of Eq. 6.4:

$$\left(\frac{d}{2}\right)^3 \int_{\eta_{i1}}^{\eta_{i2}} \left(\xi_o^2+\eta^2\right)^{\frac{1}{2}} S_{mn}(\eta)d\eta \int_{\eta_{j1}}^{\eta_{j2}} \left(\xi_o^2+\eta^2\right)^{\frac{1}{2}} S_{mn}(\eta)d\eta .$$

(6) RADIATION IMPEDANCE FOR THE ELEMENTS OF A CYLINDRICAL TRANSDUCER IDEALIZED AS AN OBLATE SPHEROID.

(9) A Technical Report

Prepared

for

The Department of the Navy
Office of Naval Research
Under Contract Nonr-2739(00)
(15)

by

(10) Richard V. Waterhouse

(11) 8 April 1960

(12) 25 p.



CAMBRIDGE ACOUSTICAL ASSOCIATES, INC.
1278 Massachusetts Avenue
Cambridge 38, Massachusetts



mt

TABLE OF CONTENTS

# RADIATION IMPEDANCE FOR THE ELEMENTS OF A CYLINDRICAL TRANSDUCER IDEALIZED AS AN OBLATE SPHEROID

## 1. Introduction

The transducer in question has the form of a right circular cylinder; the radiating elements of the transducer correspond to the curved surface of the cylinder, and the plane surfaces of the cylinder correspond to the top and bottom of the transducer, which are covered by rigid plates and are assumed to have no motion. The transducer elements have square, plane faces and form a mosaic; the total radiating surface comprises several hundred elements. Each element can be driven separately, and the problem is to calculate the mutual radiation impedance between any two elements, situated at arbitrary positions. From this information the impedance when more than one element is driven can be found easily by superposition.

The problem is one of a large group of problems which consist of calculating the mutual impedance of two sources placed in various environments. For example, the sources may be (a) in a free field,[1] (b) in the half-space above a rigid reflecting plane, (c) on the surface of such a plane,[2,3,4] (d) on the surface of a rigid sphere,[5] (e) on the surface of a rigid infinite cylinder.[6,7]

The sources may be of monopole, dipole, piston or other type, and thus the number of problems involved is quite large; the references cited give some results for these problems that have appeared in the literature.

The present problem involves calculating the near sound field of the cylindrical transducer when any one element is driven. However, there exist no exact solutions for the near sound field of a finite cylinder, and the approximate solutions[6,8] involve mathematical forms whose computation would require a very large effort.

---

1 Rayleigh, Collected Papers (Cambridge University Press, London, 1912), Vol 5, p. 137

2 S. J. Klapman, J. Acoust. Soc. Am. 11, 289, 1940

3 R. L. Pritchard, Tech. Memo. No. 21, Appendix C, Acoustics Research Laboratory, Harvard University, NR-014-903 (Jan. 15, 1951)

4 R. V. Waterhouse, J. Acoust. Soc. Am. 30, 4, (1958)

5 C. H. Sherman, J. Acoust. Soc. Am. 31, 947, (1959)

6 D. T. Laird and H. Cohen, J. Acoust. Soc. Am. 24, 46, 1952

7 D. H. Robey, J. Acoust. Soc. Am. 27, 706, (1955)

8 W. E. Williams, Proc. Camb. Phil. Soc. 52, Part 2, 322, 1956

It is therefore considered more expedient to represent the cylindrical transducer as an oblate spheroid, in which coordinate system an exact solution for the near field is available, although the functions involved are not well tabulated. This representation by a spheroid is expected to give more accurate results than the representation by a sphere which has been studied by Sherman[5] at the U. S. Navy Underwater Sound Laboratory at New London, Connecticut.

Thus the problem to be solved is the boundary value one of a quasi-rectangular source situated on the surface of a rigid oblate spheroid; as far as is known this problem has not been treated before. The source configuration is described as quasi-rectangular as it is the portion of surface of the spheroid bounded by the orthogonal coordinate lines; this surface approximates, but is not identical to, a plane rectangle as discussed further in Section 2.

## 2. Comparison of Transducer Element and Surface Element of Spheroid

The transducer is shown schematically in Fig. 1. Its height is $3.9\lambda$ and its diameter $11.4\lambda$; there are $7\times68=476$ mosaic elements, each of which has a $\lambda/2$ square radiating face.

A surface element on the spheroid, $\Delta\eta\Delta\phi$, is bounded equatorially by the parallel, curved, coordinate lines $\eta_{i1},\eta_{i2}$, where $\eta_{i1}-\eta_{i2}=\Delta\eta$, and vertically by the nonparallel, curved, coordinate lines $\phi_{i1},\phi_{i2}$, where $\phi_{i1}-\phi_{i2}=\Delta\phi$. The surface element is not plane. Such an element will be used to represent the plane, square surface of a transducer element, see Fig. 5.

There are seven rows of elements comprising the transducer; however, by symmetry only the four elements numbered 1 to 4 in Fig. 1 are needed to characterize the pressure field. The pressure field over the spheroid will be calculated for each of the four elements driven separately.

There are three main differences between the spheroid elements $\Delta\eta\Delta\phi$ and the transducer elements they represent, and these will be discussed in turn. These differences are greatest for the top row of elements, containing element 1 in Fig. 1.

a. The spheroid elements exceed the transducer elements in surface area, the largest difference being in the top row where for $\xi=0.60$ the areas are in the ratio of approximately 1.8:1; for $\xi=0.80$ the ratio is

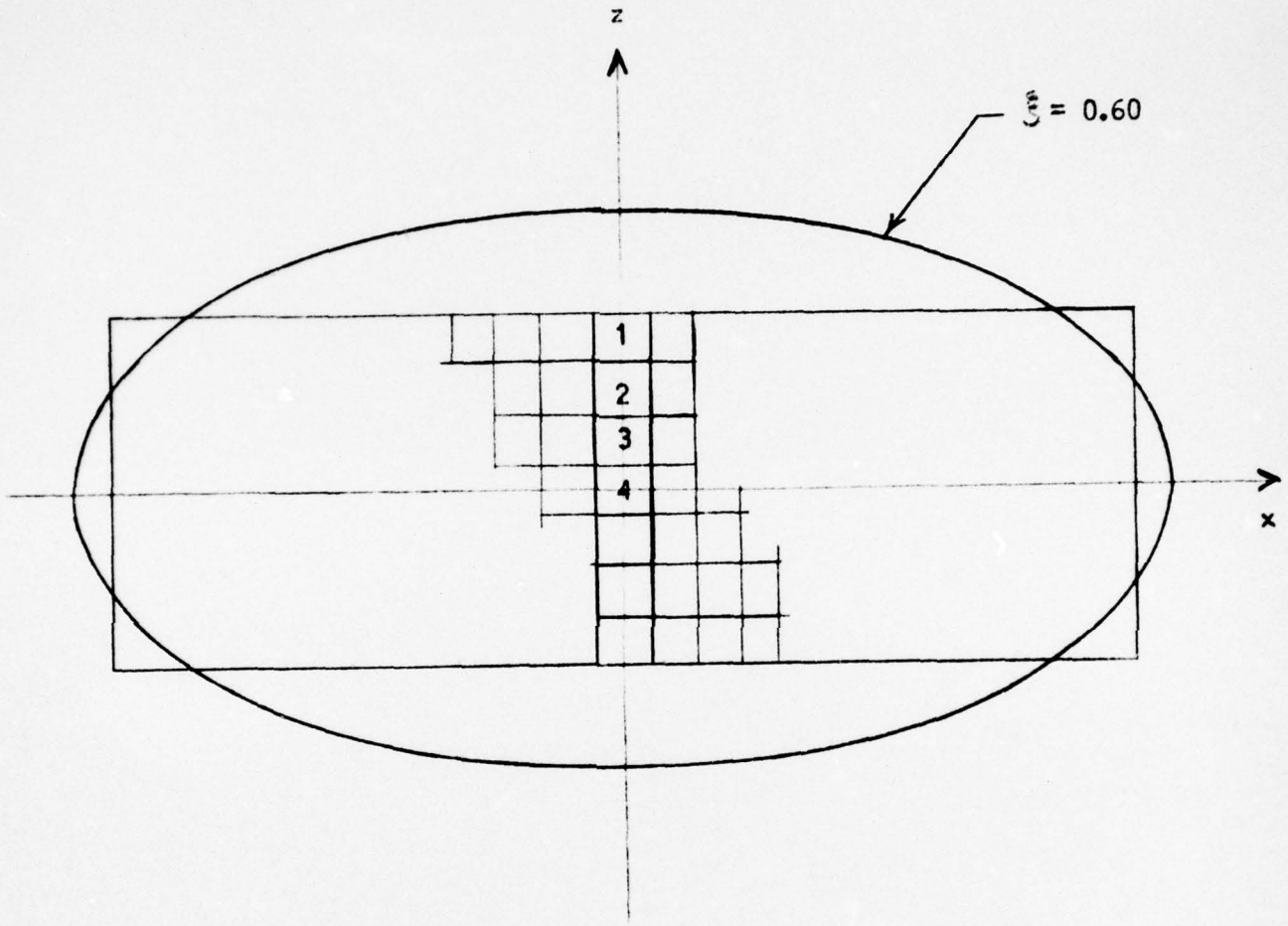


Fig. 1 Schematic diagram showing cross section of transducer (rectangular) with square mosaic elements, and of the oblate spheroid representing it.

approximately 1.4 to 1. This area difference will affect the results in which the pressure is integrated over the surface element, as in 8.1. It would be possible to compensate for this area difference by taking the spheroid surface for position 1 to be less than the projected area of the transducer element, i.e., taking the angular coordinate $\eta_{11}$ corresponding to the transducer edge to be slightly closer to the equator of the spheroid than before. However, this change would also make the element less square, and more elongated, and would affect the boundary condition (6.1). Thus it is probably better not to make this correction.

b. The nonparallel coordinate lines $\phi_{i1}, \phi_{i2}$ represent the vertical, parallel boundaries of the transducer element, and the nonparallelism is greatest for the top row of elements.

c. The coordinates lines $\eta_{i1}, \eta_{i2}$ representing the longitudinal edges of the transducer element are unequal in length. The difference is greatest for the top row of elements, where it is approximately 13 % for $\zeta = 0.60$.

The above differences between the element of spheroid surface and the transducer element it represents will cause the results to deviate slightly from those applying to a cylindrical transducer. However, this is the price paid for the relative convenience of using this coordinate system for which exact solutions to the wave equation can be written down.

## 3. Choice of Spheroid to Represent Transducer

In choosing the spheroid that will best represent the circular cylinder, a compromise has to be made. Figs. 1 and 2 show the ellipses and rectangle which are the cross sections of the spheroids and cylinder; rotation about the z axis gives the 3-dimensional figures. The equatorial portion of the spheroid corresponding to the vibrating surface of the transducer is that contained within the two long sides of the rectangle. If the spheroid chosen has a polar diameter nearly equal to the height of the transducer, the portion of the spheroid corresponding to the radiating surface of the transducer is too large and very curved, and the normal motion of the spheroid element will not represent closely the normal motion of the cylinder element.

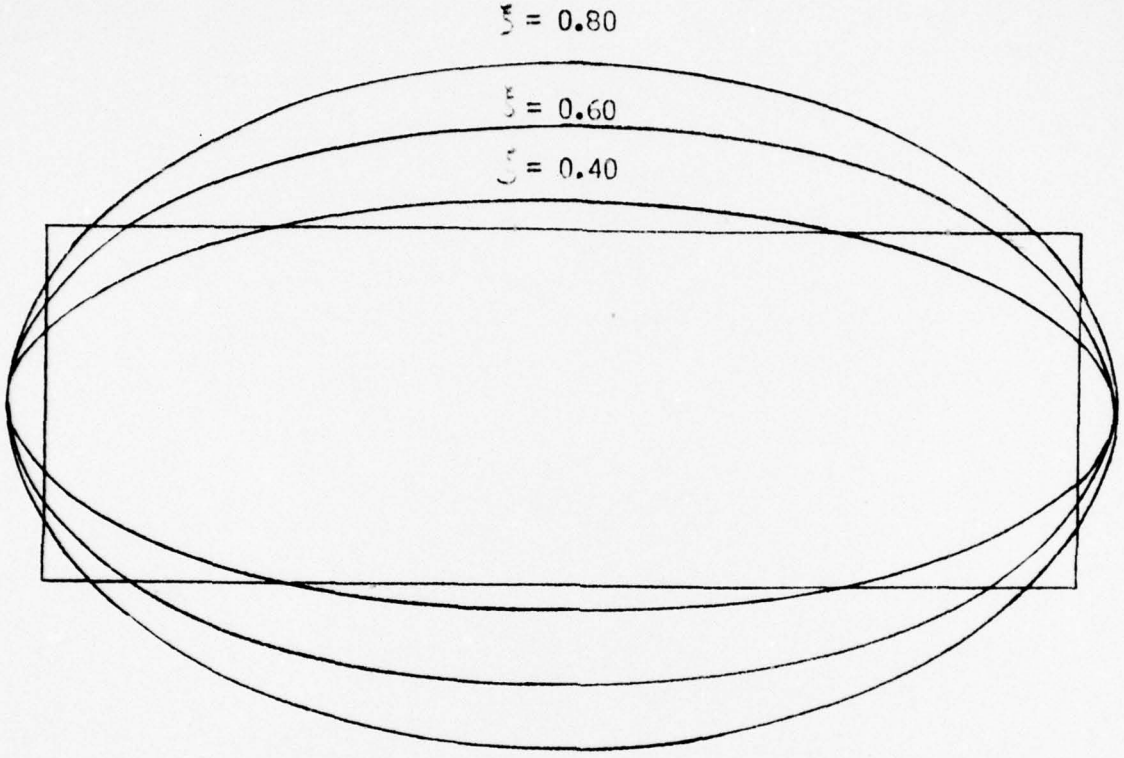


Fig. 2 Cross section of transducer and three oblate spheroids.

However, if the polar diameter of the spheroid is made large, so that the part corresponding to the radiating surface is more nearly parallel to the latter, the discrepancy between polar diameter and cylinder height becomes larger; also in this case the spheroid approaches a sphere, for which the corresponding results are already known.[5] Thus a compromise must be made between the fit at the vibrating surface and the fit at the ends of the transducer.

A factor bearing on the degree of nonparallelism tolerable between the vibrating surface of the cylinder and the corresponding surface of the spheroid, is the directional pattern of the transducer element. In the present case the element is $\lambda/2$ square, and thus its far field radiation is not highly directional,[9] as shown in Fig. 3. This implies that the results will not be sensitive to this nonparallelism, as they would be if the elements were highly directional.

In the light of all these factors, the spheroid whose proportions are specified by the value $\xi_0=0.6$ is considered a satisfactory compromise, and this value is used in the following discussion. However, another value of $\xi_0$ could be chosen without causing any significant changes in the mathematical approach in this report. The spheroid corresponding to $\xi_0=0.6$ is shown in Fig. 1; its major/minor axes are in the ratio 1.9 to 1. It thus differs appreciably from a sphere. The minor axis of the spheroid = 1.61 x the height of the transducer, and the normals to the spheroid surface at the points corresponding to the edges of the transducer are inclined at $\simeq 57^{\circ}$ to the x axis, see Fig. 4.

The length of the rectangle was taken as 0.935 of the long axis of the spheroid; this was considered to give a better match at the vibrating surface than taking it the same length as the long axis. This value tends to minimize the average difference between the separation of two elements on the transducer and on the spheroid. The values of the relevant parameters for spheroids of various proportions are given in Table 1, and Fig. 2 shows sections of spheroids corresponding to $\xi_0=0.4$ and 0.8. If the problem is of sufficient interest to justify the computing time needed, results could be computed for more than one spheroid.

---

9 H. Olson, Elements of Acoustical Engineering (Van Nostrand Co., N. Y., 2nd edition) p.32

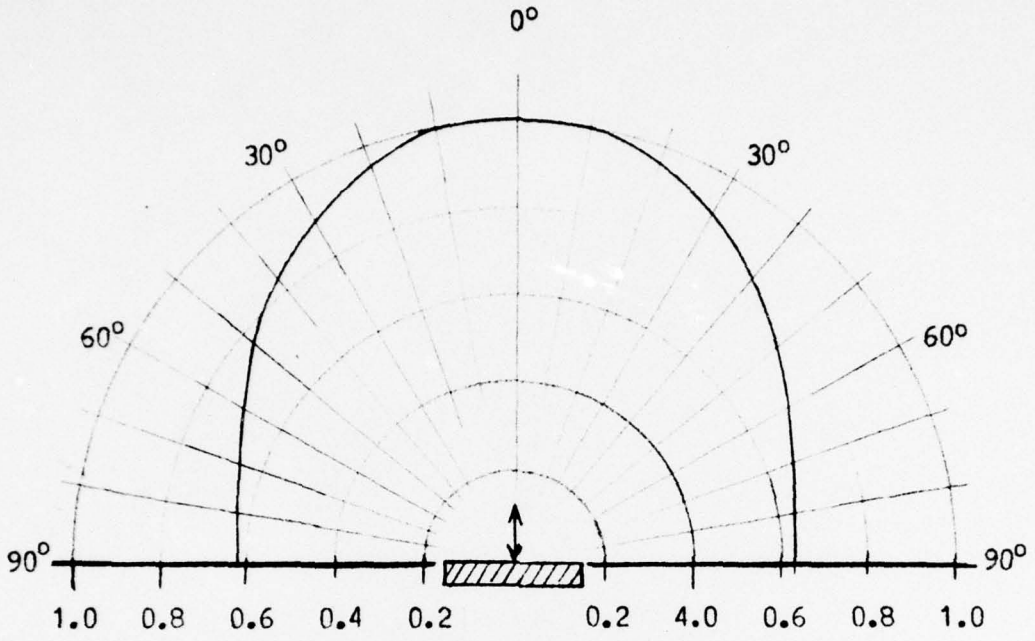


Fig. 3 Directional pattern of a plane, square piston vibrating in an infinite rigid baffle. Graph shows relative pressure as a function of polar angle in a plane parallel to the direction of motion of the piston and parallel to one of its sides. See Ref. 9.

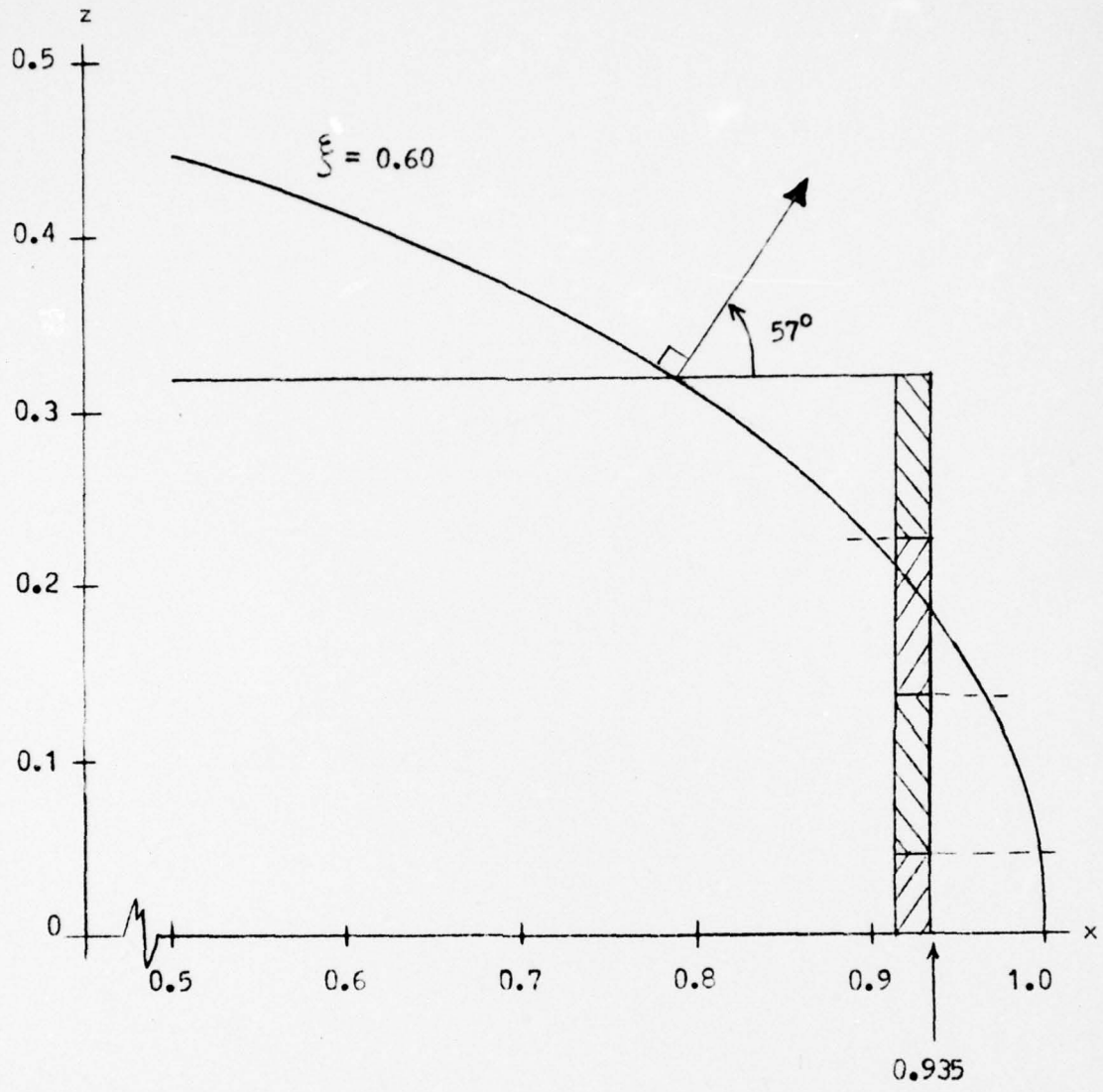


Fig. 4 Cross section of one corner of transducer showing positions of mosaic elements and corresponding part of spheroid.

TABLE 1

| $\xi$ | Frequency parameter c | Polar diameter / transducer height | Inclination to x axis of normal at edge of transducer |
|---|---|---|---|
| .4 | 35.6 | 1.16 | 78° |
| .5 | 34.2 | 1.39 | 66° |
| .6 | 32.8 | 1.61 | 57° |
| .7 | 31.3 | 1.79 | 50° |
| .8 | 29.9 | 1.95 | 44° |
| .9 | 28.4 | 2.08 | 39° |
| 1.0 | 27.1 | 2.21 | 35° |

Parameters of various oblate spheroids which could be used to represent the cylindrical transducer

4. Oblate Spheroidal Coordinates

These coordinates are obtained from elliptical coordinates by rotating them about the minor axis of the ellipse. They are obtained from rectangular coordinates by the transformation

$$x = \frac{d}{2}\left[(1-\eta^2)(\xi^2+1)\right]^{\frac{1}{2}} \cos\phi \tag{4.1}$$

$$y = \frac{d}{2}\left[(1-\eta^2)(\xi^2+1)\right]^{\frac{1}{2}} \sin\phi \tag{4.2}$$

$$z = \frac{d}{2}\eta\xi. \tag{4.3}$$

The coordinate system is represented in Fig. 5; the symbols are defined in the list of symbols, and the notation follows that of Flammer.[10] The surface $\xi$ = constant is the surface of an oblate spheroid; the surface $\eta$ = constant is a rectangular hyperboloid of two sheets; the surface $\phi$ = constant is a plane containing the z axis, see Fig. 5.

10 C. Flammer, "Spheroidal Wave Functions," Stanford University Press, Stanford, Cal. (1957)

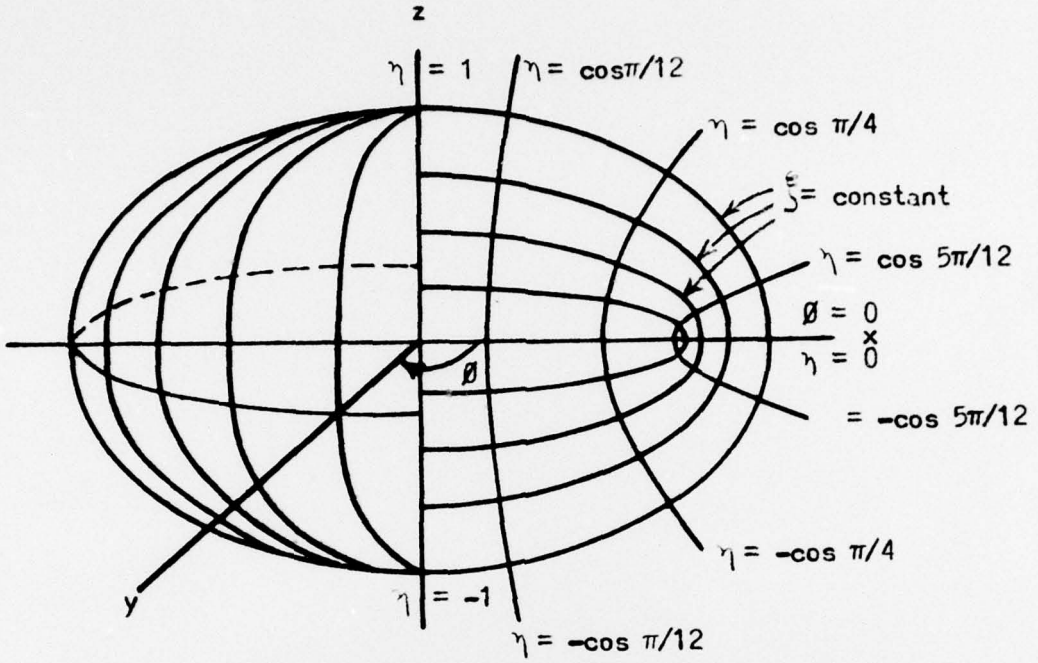


Fig. 5 Oblate spheroidal coordinate system

## 5. Solution of Wave Equation in Spheroidal Coordinates

Oblate spheroidal coordinates are one of the eleven coordinate systems in which the wave equation is separable. When sinusoidal time-dependence is assumed, the wave equation reduces to the Helmholtz equation, whose solution in oblate spheroidal coordinates for diverging waves is

$$\psi(\xi,\eta,\phi) = \sum_{m,n} a_{mni}\, R^{(3)}_{mn}(-ic, i\xi)\, S_{mn}(-ic,\eta) \begin{matrix}\cos\\ \sin\end{matrix} m\phi \qquad (5.1)$$

The symbols are defined in the list of symbols; the notation follows that of Flammer.[10] $S_{mn}(-ic,\eta)$ is an angular function; and $R^{(3)}_{mn}(-ic, i\xi)$ is a radial function. We can neglect the angular functions of the 2nd kind, $S^{(2)}_{mn}$, which tend to infinity at the poles, $\eta = \pm 1$, where we require $\psi$ to be finite. All the angular functions of $\eta$ used here will be of the first kind, and will be written $S_{nm}(\eta)$, without superscript. In this problem the frequency parameter c is fixed, so we will drop it from the exhibited variables $(\eta,\phi,\xi)$ on which the radial and angular functions depend.

The coefficients $a_{mni}$ in 5.1 must now be calculated from the main boundary condition.

## 6. Boundary Condition

The main boundary condition is the Neumann one in which the normal derivative of the dependent variable in the wave equation is specified over an interior surface; i.e., the particle velocity is specified all over the spheroid.

Thus on the spheroid surface $\xi = \xi_o$ the given or prescribed normal velocity is

$$\left| v_{g\xi}(\eta,\phi) \right| = \begin{cases} u \begin{cases} \eta_{i1} \le \eta \le \eta_{i2} \\ -\phi_i \le \phi \le \phi_i \end{cases} \\ 0 \text{ elsewhere} \end{cases} \qquad (6.1)$$

This corresponds to the $i^{th}$ transducer element, at the angular position $(\eta_{i1}, \eta_{i2}, -\phi_i, +\phi_i)$, being driven with velocity u while the rest of the surface remains motionless. The element has angular dimensions $2\phi_i$ in longitude, $(\eta_{i1} - \eta_{i2})$ in latitude, where i=1 to 4 specifies which of the

four transducer elements is excited.

Without loss of generality the element can be taken as centered on the coordinate line $\phi=0$ on the spheroid. Then since the boundary condition requires non-zero velocity at $\phi=0$, the solutions in 5.1 containing sin $m\phi$ are eliminated.

From 5.1 the velocity normal to the spheroid is

$$v_{\xi}(\eta,\phi) = \frac{1}{h_{\xi}(\eta)} \frac{\partial \psi}{\partial \xi} \tag{6.2}$$

$$= \frac{1}{h_{\xi}(\eta)} \sum_{m,\,n} a_{mni} R_{mn}^{(3)\prime}(i\xi) S_{mn}(\eta) \cos m\phi \tag{6.3}$$

In 6.2, $h_{\xi}(\eta)$ is the scale factor applying to the coordinate system and is given by

$$h_{\xi}(\eta) = \frac{d}{2}\left(\frac{\xi^2+\eta^2}{1+\xi^2}\right)^{\frac{1}{2}} \tag{6.4}$$

where d is the interfocal distance of the spheroid.

We need an expansion for the given velocity (6.1) in a series to match 6.3. However, a complication arises because the scale factor $h_{\xi}(\eta)$ in 6.3 is a function of $\eta$. If the given velocity is expanded in a series of spheroidal harmonics

$$v_{g\xi}(\eta,\phi) = \sum_{m,n} \ell_{mni} S_{mn}(\eta) \cos m\phi \tag{6.4a}$$

the coefficients $\ell_{mni}$ cannot be matched with the $a_{mni}$ in 6.3, since the latter contains $h_{\xi}(\eta)$. An expansion of the given velocity in terms of the spheroidal harmonics 6.4a divided by $h_{\xi}(\eta)$ is unfruitful, as the resulting functions do not form an orthogonal set.

The difficulty can be circumvented by expanding the product

$$h_{\xi}(\eta)\, v_{g\xi}(\eta,\phi) = \sum_{m,n} \ell_{mni} S_{mn}(\eta) \cos m\phi \tag{6.5}$$

and dividing out the scale factor later, (see 6.9). The coefficients $\ell_{mni}$ are then obtained as usual by multiplying (6.5) by $S_{mn}(\eta)\cos m\phi$ and integrating. We define an integral

$$I_{mni} = \int_{-1}^{1} \int_{0}^{2\pi} h_\xi(\eta)\, v_{g\xi}(\eta,\emptyset)\, S_{mn}(\eta) \cos m\emptyset \, d\eta \, d\emptyset \tag{6.6}$$

$$= \ell_{mni} \int_{-1}^{1} S_{mn}^2(\eta)\, d\eta \int_{0}^{2\pi} \cos^2 m\emptyset \, d\emptyset \tag{6.7}$$

$$= \ell_{mni}\, N_{mn}\, \pi \tag{6.8}$$

where $N_{mn}$ is the norm of $S_{mn}(\eta)$.

Substituting for $\ell_{mni}$ from 6.8 into 6.5 and rearranging,

$$v_{g\xi}(\eta,\emptyset) = \frac{1}{h_\xi(\eta)} \sum_{m,n} \frac{I_{mni}}{\pi N_{mn}} S_{mn}(\eta) \cos m\emptyset \tag{6.9}$$

which must equal 6.3; the coefficients in 6.3 and 6.9 can now be equated without difficulty, giving

$$a_{mni} = \frac{I_{mni}}{\pi\, N_{mn}\, R_{mn}^{(3)'}(i\xi_0)} \tag{6.10}$$

When these coefficients $a_{mni}$ are evaluated and inserted in (5.1) the pressure at any field-point can be calculated. We note that since the driven element occupies only some $5^\circ$ out of the $180^\circ$ range, many terms in the expansion 6.9 will be needed to represent it accurately.

Inserting the boundary condition 6.1 in 6.8,

$$I_{mni} = u \int_{\eta_{i1}}^{\eta_{i2}} h_\xi(\eta)\, S_{mn}(\eta)\, d\eta \int_{0}^{\emptyset_i} 2 \cos m\emptyset \, d\emptyset \tag{6.11}$$

$\eta_{i1}, \eta_{i2}$ and $\emptyset_i$ will vary with the position of the source element. The integration with respect to $\emptyset$ can be performed directly, yielding

$$I_{mni} = \frac{2u}{m} \sin(m\emptyset_i) \int_{\eta_{i1}}^{\eta_{i2}} h_\xi(\eta)\, S_{mn}(\eta)\, d\eta \tag{6.12}$$

The computation of $I_{mni}$ from this expression, and hence of $a_{mni}$ in 6.10, is discussed in Section 10c.

## 7. Near-field Pressure

The pressure at any field-point is given by

$$p_i(\xi,\eta,\phi) = -\rho \frac{\partial \psi_i}{\partial t} \tag{7.1}$$

$$= i\rho\omega \sum_{m,n} a_{mni} S_{mn}(\eta) R^{(3)}_{mn}(i\xi) \cos m\phi \tag{7.2}$$

from 5.1, since the time dependence is given by $\exp(-i\omega t)$. Now on the surface of the spheroid $\xi = \xi_o$, and $\rho$, $\omega$, $c$, $\xi_o$ are constants for this problem, $R^{(3)}_{mn}(i\xi_o)$ is fixed for each mode mn and the coefficients $a_{mni}$ are calculable as shown in Section 10c. Thus

$$\sum_{m,n} p_{mni}(\xi_o,\eta,\phi) = i\rho\omega \sum_{m,n} a_{mni} R^{(3)}_{mn}(i\xi_o) S_{mn}(\eta) \cos m\phi \tag{7.3}$$

This gives the pressure as a function of position $(\eta, \phi)$ on the spheroid surface, due to the excitation of the $i^{th}$ transducer element. The calculation of the pressure field from 7.3 is discussed in Section 10.

## 8. Mutual Impedance Between Two Elements

The pressure field due to the $i^{th}$ element, given by 7.3, is now integrated over the surface of another element j, to give the mutual impedance $Z_{ij}$ between the two elements.

$$Z_{ij} = \frac{1}{u} \int_{\eta_{j1}}^{\eta_{j2}} \int_{\phi_{j1}}^{\phi_{j2}} p_{mni}(\eta,\phi)\, d\eta\, d\phi \tag{8.1}$$

Substituting for $\sum_{m,n} p_{mni}$ from 7.3, and performing the integration with respect to $\phi$, 8.1 becomes

$$Z_{ij} = i\frac{\rho\omega}{u} \sum_{m,n} \left\{ a_{mni} \frac{R^{(3)}_{mn}(i\xi_o)}{m} \left[\sin m\phi_{j1} - \sin m\phi_{j2}\right] \int_{\eta_{j1}}^{\eta_{j2}} S_{mn}(\eta)\, d\eta \right\} \tag{8.2}$$

Substituting for $a_{mni}$ from 6.10 and 6.12, we obtain

$$Z_{ij} = \frac{i2\rho\omega}{\pi} \sum_{m,n} \left\{ \frac{\sin m\phi_i}{m^2 N_{mn}} \left(\sin m\phi_{j1} - \sin m\phi_{j2}\right) \cdot \frac{R^{(3)}_{mn}(i\xi_o)}{R^{(1)\prime}_{mn}(i\xi_o)} \cdot \int_{\eta_{i1}}^{\eta_{i2}} S_{mn}(\eta) S_{mn}(\eta)\, d\eta \int_{\eta_{j1}}^{\eta_{j2}} S_{mn}(\eta)\, d\eta \right\} \tag{8.3}$$

This gives the mutual impedance between the $i^{th}$ and $j^{th}$ elements of the transducer. The calculation of these mutual impedances is discussed in Section 10. The number of different values of $Z_{ij}$ needed to specify this quantity for every element of the transducer is 544, as discussed in Section 9.

The total radiation impedance imposed on the $j^{th}$ element when an arbitrary number N of other elements are being driven is found by superposition to be

$$Z_j = \frac{1}{u_j} \sum_{i=1}^{N} Z_{ij} u_i \tag{8.4}$$

where the $i^{th}$ source is driven with velocity $u_i$ .

## 9. Degeneracy of $Z_{ij}$

The transducer consists of 7 rows and 68 columns of elements, comprising 476 elements in all. The question arises as to how many different values are needed to specify the mutual impedance $Z_{ij}$ between every pair of elements i and j.

First we note that by reciprocity

$$Z_{ij} = Z_{ji} \tag{9.1}$$

This reduces the number of different values of $Z_{ij}$, but even so if the transducer possessed no spatial symmetry of any kind, the number of different values would be 476 (1 + 476/2) = 113,764, a large number.

In fact the transducer has rotational symmetry about its axis and mirror symmetry about its equatorial plane, and the different values of $Z_{ij}$ for the four source elements and any column of (7) elements are given in Table 2.

TABLE 2

| | | | | | | |
|---|---|---|---|---|---|---|
| $Z_{11}$ | . | . | . | . | . | . |
| $Z_{12}$ | $Z_{22}$ | . | . | . | . | . |
| $Z_{13}$ | $Z_{23}$ | $Z_{33}$ | . | . | . | . |
| $Z_{14}$ | $Z_{24}$ | $Z_{34}$ | $Z_{44}$ | . | . | . |
| $Z_{15}$ | $Z_{25}$ | $Z_{35}$ | . | . | . | . |
| $Z_{16}$ | $Z_{26}$ | . | . | . | . | . |
| $Z_{17}$ | . | . | . | . | . | . |

In this Table the first digit of each subscript specifies the position of the source element, and has the range 1 to 4, see Fig. 1. The second digit specifies the row of the other element, and has the range 1 to 7. From considerations of symmetry, it is found that for the four source positions and any one column of elements, there exist 16 different values of $Z_{ij}$. Each dot in Table 2 represents a value of $Z_{ij}$ equal to one of the values written in, as given in Table 3.

TABLE 3

$$Z_{44}$$

$$Z_{33} = Z_{55} \qquad Z_{17} = Z_{71}$$

$$Z_{22} = Z_{66} \qquad Z_{35} = Z_{53}$$

$$Z_{11} = Z_{77} \qquad Z_{26} = Z_{62}$$

$$Z_{12} = Z_{21} = Z_{67} = Z_{76}$$

$$Z_{13} = Z_{31} = Z_{57} = Z_{75}$$

$$Z_{14} = Z_{41} = Z_{47} = Z_{74}$$

$$Z_{15} = Z_{51} = Z_{37} = Z_{73}$$

$$Z_{16} = Z_{61} = Z_{27} = Z_{72}$$

$$Z_{23} = Z_{32} = Z_{56} = Z_{65}$$

$$Z_{24} = Z_{42} = Z_{46} = Z_{64}$$

$$Z_{25} = Z_{52} = Z_{36} = Z_{63}$$

$$Z_{34} = Z_{43} = Z_{54} = Z_{45}$$

There are 68 columns of elements in the transducer, of which 34 will yield different values of $Z_{ij}$, by symmetry. The total number of different values of $Z_{ij}$ existing for the transducer is therefore 16x34=544.

In the general case of a transducer of this shape and symmetry having N rows and M columns, (M,N>2) the number is the product of (1+3+5+...N) or (2+4+6+...N) for N odd or even respectively, and (M-1)/2 or M/2 for M odd or even, respectively. It may be noted that M and N are not interchangeable in these expressions; that is because the vertical

symmetry (mirror) and the horizontal symmetry (circular) are different.

For the transducer shown in Fig. 1, in addition to the 544 different values of $Z_{ij}$ there are also four different values of self-impedance $Z_i$, one for each of the four distinct source positions.

10. Computation Required

It is desired to calculate values of $\sum_{m,n} p_{mni}$, and $Z_{ij}$ for the various transducer elements. This requires both calculation of the spheroidal functions, which are not tabulated in the range required, as well as the numerical evaluation of certain integrals. A discussion of the scope of this work is given in the following sections.

10a. Angular Functions

In the present case the transducer is 11.4λ in diameter, and the corresponding frequency parameter c for the spheroid has the relatively large value of 32.8. None of the existing tables of spheroidal functions[10,11,12] extend to such high values of c, and thus the required angular and radial functions must be computed.

Flammer gives an asymptotic expansion for the angular functions that is valid when $c\xi$ is large, as in the present case where $c\xi = 19.68$; see Ref. 10, pp 62-7, equations (8.2.9) to (8.2.42). The expansion is in terms of the associated Laguerre polynomials, and should give an easier computing task than the usual, non-asymptotic expansion.

We require $S_{mn}(-32.8i,\eta)$ for $\eta$ going from 0 to $\simeq 0.65$; for the lower modes, only a few values of $\eta$ will be required to define the function accurately over the range; for the higher modes more values of $\eta$ will be needed. The resulting values of $S_{mn}(\eta)$ will be used first in 6.12 to evaluate the expansion coefficients specifying the boundary condition and then again in 7.3 to obtain the pressure at a field point.

It is not known at present how many modes will be required to fit to the boundary conditions with reasonable accuracy; however, since the transducer element has an angular width of some $5.4^\circ$ which is $\simeq 1/33$ of the $180^\circ$ range from pole to pole of the spheroid, it seems probable by considering the corresponding Fourier expansion that not less than 30 harmonics would be needed to provide accuracy of the order of 10 %.

---

11 J. A. Stratton, P. M. Morse, L. J. Chu and R. A. Hutner, Elliptic Cylinder and Spheroidal Wave Functions, John Wiley and Sons (1941).

12 J. A. Stratton, P. M. Morse, L. J. Chu, J. D. C. Little, F. J. Corbató, Spheroidal Wave Functions, John Wiley and Sons (1956).

The norm $N_{mn}$ of the angular functions is required in 6.10. On p. 67 of Ref. 10 an asymptotic expression $\mathfrak{N}_{mn}$ for this quantity is discussed.

10b. Radial Functions

The pressure is needed only on the surface of the spheroid, thus only one value of the radial function, and one of its derivative need be calculated for each mode. Since $\xi_0=0.6$, and $c=32.8$, $c\xi_0=19.68$, and the latter value is large enough for the following asymptotic expression[13] to be used:

$$R_{mn}^{(3)}(-ic, i\xi) \xrightarrow[c\xi\to\infty]{} \frac{1}{c\xi} \exp i\left[c\xi - \frac{1}{2}(n+1)\pi\right] \qquad (10.1)$$

The real part of this radial function corresponds to the pressure component in phase with the velocity, and the imaginary part to that out of phase.

The asymptotic expression for the derivative of the radial function can be obtained directly from 9.1 by differentiating:

$$R_{mn}^{(3)'}(ic, i\xi) = \frac{(ic\xi - 1)}{c\xi^2} \exp i\left[c\xi - \frac{1}{2}(n+1)\pi\right] \qquad (10.2)$$

Thus from 10.1 and 10.2 the ratio of the radial function to its derivative, as required in 8.3 is

$$\frac{R_{mn}^{(3)}}{R_{mn}^{(3)'}} = \xi/(ic\xi - 1) \qquad (10.3)$$

10c. Expansion Coefficients

In 6.10 the expansion coefficients $a_{mni}$ for a mode mn and position i of the transducer element are given in terms of an integral $I_{mni}$ defined in 6.12. $I_{mni}$ may be calculated as follows:

1) From 6.4 $h_\xi^{(\eta)}$ is calculated over the range $\eta=0$ to $\eta=\eta_{11}$, where $\eta_{11}$ corresponds to the half-height of the transducer. The same function $h_\xi^{(\eta)}$ will be used for all modes.

2) $S_{mn}(\eta)$ is obtained as discussed in 10a.

3) From (1) and (2) the product $h_\xi^{(\eta)}\ S_{mn}(\eta)$ is then formed for each mode mn.

4) The integral in 6.12 is required, and this is obtained numerically for each mode mn over the ranges $\eta_{i1}$-$\eta_{i2}$, i = 1 to 4; this yields 4 mn values.

5) Each of the values obtained in (4) is multiplied by $\frac{2u}{\pi}\sin m\phi_i$,

---

13 Flammer in Ref. 10 gives 10.1 incorrectly on p. 67, Eq. (8.2.48) as the limit as $\xi\to\infty$, but correctly on p. 32, Eq. (4.1.17) as limit when $c\xi \longrightarrow \infty$.

yielding 4mn values of $I_{mni}$. The factor u can be carried through as a symbol; it will go out when the expression for $Z_{ij}$ (8.2) is calculated.

Having found these values of $I_{mni}$, $a_{mni}$ is obtained from 6.10, $R_{mn}^{(3)'}(\xi_o)$ having been obtained as in Section 10b, and $N_{mn}$ as in Section 10a. There are 4mn values of $a_{mni}$.

10d. Calculation of Pressure at Transducer Surface

Following the scheme of calculation given in 10a, b and c, $\sum_{mn} p_{mni}(\eta,\emptyset)$ as given in 7.3 is now calculable as a function of angular position $(\eta,\emptyset)$ on the spheroid, using as many modes as are needed. $Z_{ij}$ is then calculated from 8.1, evaluating the integral numerically.

## List of Symbols

$a_{mni}$ = numerical coefficient for mn mode, in expansion of sound field produced by driving the $i^{th}$ transducer element

$c$ = frequency parameter, = kd/2

$c_o$ = sound velocity

$d$ = interfocal distance of spheroid

$h_\xi(\eta)$ = coordinate scale factor

$i, j$ = transducer elements

$I_{mni}$ = integral defined in (6.6)

$k$ = wave number, = $\omega/c_o$

$\ell_{mni}$ = numerical coefficient in expansion of boundary condition

$m, n$ = numbers specifying the vibrational mode

$M, N$ = integers > 2

$N_{mn}$ = norm of $S_{mn}(\eta)$

$p_i$ = pressure field radiated by $i^{th}$ element

$p_{mni}$ = pressure of mn mode radiated by $i^{th}$ element

$R_{mn}^{(3)}(-ic, i\xi)$ = radial function of the $3^{rd}$ kind, of order m and degree n

$R_{mn}^{(3)\prime}(-ic, i\xi)$ = derivative of $R_{mn}^{(3)}(-ic, i\xi)$ with respect to $\xi$.

$S_{mn}(\eta)$ = angular function of the $1^{st}$ kind, of order m and degree n

$t$ = time

$u$ = velocity amplitude of driven transducer element

$u_i, u_j$ = velocity of $i^{th}$ and $j^{th}$ elements

$v_\xi$ = velocity normal to spheroid surface

$v_{g\xi}$ = given velocity normal to spheroid surface

$x, y, z$ = rectangular coordinates

$Z_{ij}$ = mutual impedance between elements i and j

$Z_j$ = radiation impedance of $j^{th}$ element

$\eta$ = angular coordinate

$\eta_{i1}, \eta_{i2}$ = angular coordinates defining the upper and lower sides of the $i^{th}$ element

$\eta_{11}$ = angular coordinate defining upper side of element in position 1, Fig. 1

$\lambda$ = wavelength

$\xi, \xi_o$ = radial coordinate

$\rho$ = fluid density

$\phi$ = angular coordinate

$\phi_{i1}, \phi_{i2}$ = angular coordinates defining the vertical sides of the $i^{th}$ element

$-\phi_i, +\phi_i$ = angular coordinates defining the vertical sides of the $i^{th}$ element when i=1 to 4, Fig. 1

$\Psi$ = velocity potential

$\Psi_i$ = velocity potential caused by radiation of $i^{th}$ element

$\omega$ = $2\pi$ x frequency

DISTRIBUTION LIST

Office of Naval Research (Code 411)
Department of the Navy
Washington 25, D. C. (7 copies)

Director
Naval Research Laboratory
Technical Information Officer
Washington 25, D. C. (1 copy)

Director
Naval Research Laboratory
Sound Division
Washington 25, D. C. (1 copy)

Commanding Officer
Office of Naval Research Branch Office
The John Crerar Library Building
86 East Randolph Street
Chicago 1, Illinois (1 copy)

Commanding Officer
Office of Naval Research Branch Office
495 Summer Street
Boston 10, Mass. (1 copy)

Commanding Officer
Office of Naval Research Branch Office
Navy No. 100, Fleet Post Office
New York, N. Y. (1 copy)

Commanding Officer and Director
U. S. Navy Underwater Sound Laboratory
Fort Trumbull
New London, Conn. (1 copy)

Commander
Naval Ordnance Laboratory
White Oak
Silver Spring, Maryland (1 copy)
(Attn: Acoustics Division)

Commanding Officer and Director
U. S. Navy Electronics Laboratory
San Diego 52, California (1 copy)

Commanding Officer
U. S. Naval Mine Defense Laboratory
Panama City, Florida (1 copy)

Commander
U. S. Naval Air Development Center
Johnsville, Pennsylvania (1 copy)

Commanding Officer and Director
David Taylor Model Basin
Washington 7, D. C. (1 copy)

Director
U.S. Navy Underwater Sound Reference Laboratory
Office of Naval Research
P. O. Box 3629
Orlando, Florida (1 copy)

Contract Administrator S.E. area
Office of Naval Research
2110 G Street N. W.
Washington 7, D. C. (1 copy)

Hudson Laboratories
Columbia University
145 Palisades Street
Dobbs Ferry, N. Y.

Lamont Geological Observatory
Columbia University
Torre Cliffs
Palisades, N. Y.

Brown University
Research Analysis Group
Providence, R. I.

Woods Hole Oceanographic Institution
Woods Hole, Massachusetts